17th World Conference on Earthquake Engineering, 17WCEE
Sendai, Japan - September 13th to 18th 2020

8-SHAPED FLOATING DAMPING DEVICE AGAINST SLOSHING FOR WATER TANK TO IMPROVE EARTHQUAKE RESISTANCE

T. Ono [1], T. Ida [2], H. Hirano [3], N. Sato [4]

[1] *Student, Major of Civil, Human and Environmental Science Engineering, Chuo University, a19.grk4@g.chuo-u.ac.jp*
[2] *Deputy Director, Togawa Rubber Co., Ltd. Research and Development Department, tsuyoshi-ida@togawa.co.jp*
[3] *Professor, Faculty of Policy Management, Chuo University, hirano@tamacc.chuo-u.ac.jp*
[4] *Professor, Department of Civil and Environmental Engineering, Chuo University, nsato.57n@g.chuo-u.ac.jp*
…

Abstract

In the Kumamoto earthquake and the Great East Japan Earthquake, water storage tanks which are settled in apartment houses and public buildings were damaged due to the sloshing phenomenon excited by long-period seismic motion. In several cases at important buildings such as hospitals these damages introduced serious shortage of water, resulting fatal effect. In order to prepare for large earthquakes occurring in the near future, it is necessary to grasp the dynamic behavior of the water storage tank to reduce the sloshing phenomenon in order to secure the lifeline at the time of earthquake disaster. In a previous study by the authors, the panel type vibration damping device demonstrated the effect of reducing sloshing on the water tank. However, the workability of the vibration damping device was poor, and it took a lot of time and efforts in constructions. Therefore, in this research, we improved the workability and devised a method to assemble the panel into a figure 8 shape. Experiments were carried out in a real scale water tank to verify the workability of this vibration damping device and the effect of reducing sloshing. As a result, it was found that the workability is remarkably superior to that of the conventional vibration damping device, and also the wave height reduction effect of the same level as the wave height reduction rate is exhibited as in the conventional case.

Keywords: floating damping device, sloshing, real scale tank, experimental excitation

1. Introduction

Damages have been confirmed in water tanks installed in hospitals as shown in Photo 1 in the 2016 Kumamoto earthquake. Here, since the upper side wall and the ceiling of the corner of the FRP tank were damaged, the sloshing phenomenon is considered to be the main cause of damage. Water tank damages occurred the Great East Japan Earthquake, and water tanks that are one of the important lifelines in hospitals, schools and other evacuation shelters have had an impact.

It is thought that this kind of water tank damage is one of the causes of sloshing phenomenon (excitation of liquid level fluctuation) excited by slightly long-period ground motion. Earthquakes such as Tokai, Tonankai and Nankai, which are predicted to occur in the near future might excite 2-5 seconds of slightly long-period earthquakes. Therefore, it is thought that there is a great social need to understand the dynamic behavior of a water tank.

On the other hand, understanding the dynamic behavior during an earthquake and suppressing the occurrence of fluctuations in the liquid level of the internal solution is very meaningful because it leads to the prevention of damage to the water tanks, which plays an important role as a lifeline. Various studies have been conducted on these measures, and methods such as installing a wire mesh inside the water tank, installing a resistance plate, and attaching plastic fibers to the side walls are proposed. However, when these methods are installed in existing water tanks, there are problems in workability, such as the fixing method of the equipment, as well as issues such as regular internal cleaning that is legally required to ensure hygiene. Therefore, none has been put into practical use.

Based on the above background, this paper proposes a vibration control device that can be assembled as easily as possible and constracts the panel into an 8-shaped panel in pursuit of economical and hygiene. This damping device is installed in the FRP tank which has the most installation record as a water storage tank, and the damping effect is confirmed. Specifically, we conducted a sine wave primary mode and seismic uniaxial excitation experiment using a 2×2×2m FRP tank, which is also used for improved water tanks.

Photo 1 Example of damage to the upper of the corner and the ceiling

(FRP tank) (Minami-ku, Kumamoto City)

2. 8-shaped floating damping device

In our previous research, we have demonstrated that the cross-type floating vibration damping device combined with the resistive plate panel shown in Fig. 1 is effective in reducing sloshing generated in a water tank. However, when installed in an existing tank, the shape was complicated, and the work was poor due to dimensional adjustments, which took time. Therefore, it is required that anyone can assemble damping device as easily as possible.

In order to improve workability as a top priority and pursue economy and hygiene, as shown in Photo 2, we have assembled an 8-shaped device using panels floating in the tank. In this paper, as shown in Photo 3, this is floated inside the tank and the damping effect is examined.

The mechanism of this damping device increase a resistance force by utilizing flotation when the liquid passes through the slit of the damping device. In addition, by crossing at the center of the tank, it corresponds to the direction of vibration, and a resistor is provided in the center where the velocity energy of the content liquid is maximum. And by making the shape into an 8-shaped, it is possible to handle tanks in any shapes by combining multiple 8-shaped damping devices together with the stress distribution of the damping device. The specific gravity of this material is 0.9, so it floats near the water surface. Therefore, it is effectively controlled by the movement of the fluid near the water surface, and can respond to changes in the depth of the internal solution. The damping device has a slit shape in consideration of the workability required to ensure the sanitary condition stipulated by law and the method of regular internal cleaning.

The properties of the damper panel are as follows: hardness: A94, storage modulus: 117 MPa, tensile strength: 32.3 MPa, elongation at break: 810%. This damper panel is bent into an 8-shape and joined and assembled and installed on site. These plate members are stacked vertically with a gap to form a damping device. Since the specific gravity of this material is 0.9 as described above, it floats near the water surface when water is added. This effectively suppresses sloshing, in which fluid motion near the water surface is dominant, and changes the water depth of the water tank.

After assembling the damping device outside the water tank, it is also possible to put it directly into the water tank from the manhole with a diameter of about 600mm. This is possible because of the flexibility that is one of the characteristics of this material. In this way the work in the water tank has been devised in order to reduce to a minimum. Finally, water is poured into the water tank as shown in Photo 3, and the damping device is floated to complete the construction. In the case of this construction method, the damper panel can be flexibly bent according to the dimensions of the tank, and the connecting part is simply fixed with bolts. Compared with Cross-shaped floating damping device, workability is greatly improved.

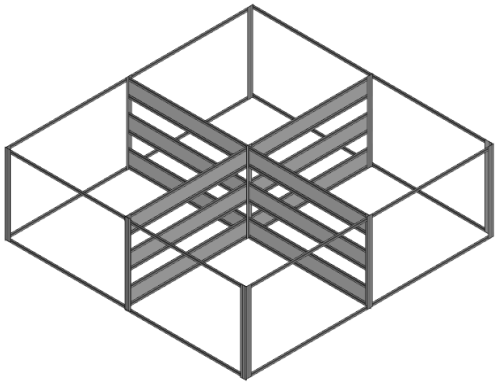

Fig. 1 Cross-shaped floating damping device

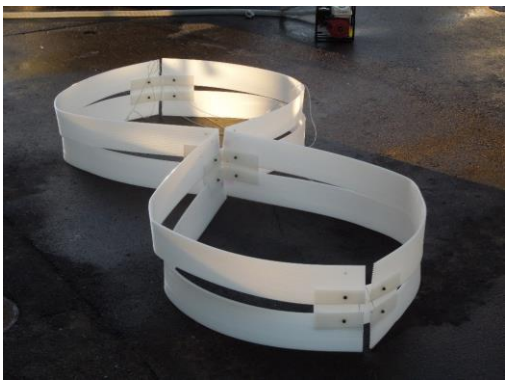

Photo 2 8-shaped floating damping device

Photo 3 Installation situation of 8-shaped floating damping device

3. Outline of the experiment

3.1 Arrangement of measuring equipment

In this paper, we use the FRP water tank used for the elevated water tank of 2000mm on each side shown in Photo 4. This is filled with water up to 1400mm, which is the depth of water during normal use, and a vibration experiment is performed. Also, as shown in Fig. 2, a laser displacement meter for wave height measurement and wall displacement measurement and a pressure gauge for dynamic fluid pressure measurement are installed on the tank wall surface to clarify the effect of the damping device.

The displacement meter uses IL-600 manufactured by KEYENCE Co., Ltd., and measures the response wave height by irradiating the target with a foamed polystyrene board floating through a wire in the tank. In order to measure the wall displacement, it is installed at the height of 500mm of the shaking table and tank wall, and the displacement is calculated. The data sampling frequency is 10Hz.

The pressure gauge uses PGM-G manufactured by Kyowa Dengyou Co., Ltd. These are installed at a total of three locations in the center of the panels with heights of 500mm, 1000mm and 1400mm shown in Fig.2. The pressure gauge measures the change in dynamic fluid pressure at each installation position. Data sampling frequency is 50Hz.

The change in fluid pressure is defined as shown in Eq. (1).

$$\Delta P = P - P_0 \tag{1}$$

Here, ΔP is the change in hydrodynamic pressure, P is the total pressure, and P_0 is the hydrostatic pressure. Thus, the hydrostatic pressure change at each pressure gauge installation position is measured by measuring the hydrostatic pressure filled with water as zero. By this method, the change of the hydraulic pressure on the wall surface when sloshing occurs is examined.

In addition, multiple waterproof web cameras are installed inside the tank to record video. Based on these results, the differences due to the presence or absence of vibration control devices are compared and examined.

Photo 4 2000mm square FRP water tank

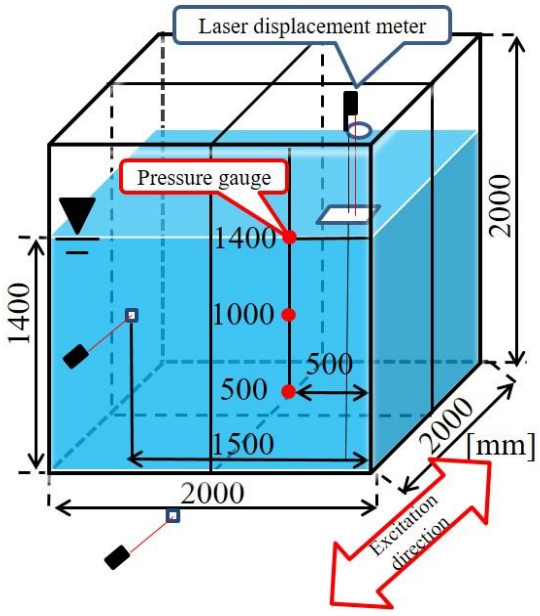

Fig. 2 Measurement equipment location

3.2 Excitation conditions

For the shaking table, a tank is installed in a large vibration device jointly established by Chuo University and Aichi Institute of Technology, and an excitation experiment is performed. The shaking table is a regular octagon of 4500mm in the east-west direction and 4500mm in the north-south direction. The vibration unit uses two 500kN actuators manufactured by MTS, the control unit uses a 4830 controller manufactured by Shimadzu Corporation, and the linear roller way super X manufactured by Nippon Thompson Co., Ltd. is used for the rails and rollers. Since this shaking table uses two actuators in synchronism, it is forcibly stopped when the stroke difference between the two actuators is ± 2.5mm and the test force difference is ± 300kN for safety. In the excitation experiment, a sine wave input excitation experiment and a seismic input excitation experiment are performed.

For the sine wave input excitation experiment, the theoretical value of the first-order mode sloshing natural frequency calculated from Housner's equation shown in Eq. (2) is used.

Here, H is depth (m), L is the tank width (m).

$$f = \frac{1}{2\pi} \cdot \sqrt{\frac{(2n-1)\cdot\pi\cdot g}{L} \cdot \tanh\left(\frac{(2n-1)\cdot\pi\cdot H}{L}\right)} \tag{2}$$

4. Experimental results

4.1 Primary mode 0.60Hz sine wave excitation

For sine wave input excitation, the input frequency is set to 0.60 Hz, which is the natural frequency of the sloshing first-order mode that maximizes the response wave height, and the input wave frequency is 10 sine waves. Set the excitation amplitude to ± 5, ± 7, ± 10 mm. Here, response wave height, wall displacement and dynamic fluid pressure are measured. The excitation conditions are summarized in Table 1.

Table 1 Excitation conditions

Inner wall width L	2000mm
Water depth H	1400mm
Input frequency	0.60Hz
Input wave number	10 waves
Excitation amplitude	±5, ±7, ±10mm

a) Response wave height

Fig. 3 shows the response wave height when the primary mode is 0.60Hz and ± 5mm. Focusing on non-damping, the maximum wave height is 238 mm. Compared with this result, by adding a damping device, the maximum wave height is 154mm and the wave height is reduced by about 35%. In addition, it can be seen from the response waveform shown in Fig. 3 that the sloshing behavior immediately after the vibration was stopped converged by adding a damping device. The maximum wave height and its damping constant are calculated from the data obtained from the displacement meter, and the comparison is made between the case of non-damping suppression and the case of addition of a damping device. The attenuation constant is calculated by comparing the waveform obtained by the free attenuation after the vibration is stopped with the attenuation curve obtained from Eq. (3).

$$\eta_d(t) = A\exp(-\omega_0 ht) \quad (3)$$

Here, η_d is the damping curve, A is the amplitude immediately after the excitation is stopped, ω_0 is the natural angular frequency, h is the damping constant, and t is the time.

At this time, the damping constant from the maximum wave height immediately after the excitation stop to the 20th wave is 0.0010 for non-vibration, whereas it is 0.010, which is about 10 times greater during damping. Thus, it was clarified that the damping constant increased and the wave height reduction effect was obtained by adding the damping device.

Similarly, Fig. 4 shows the response wave height when the primary mode is 0.60Hz and ± 7mm. The maximum wave height is 433mm. Compared with this result, the addition of a damping device shows a maximum wave height of 218mm, which is reduced by about 50%. The damping constant is 0.0015 for non-damping, while it is about 7.3 times 0.011 for damping.

Fig. 5 shows the response wave height when the primary mode is 0.60Hz and ± 10mm. Since non-vibration control is far from the measurement range of non-contact displacement meters, waveform measurement is impossible. On the other hand, when the vibration control device was installed, it was within the measurement range and showed a maximum wave height of 300 mm. The damping constant here is 0.012 during damping.

As a result, the damping constant increased by about 7 to 10 times by adding a damping device.

Fig. 6 shows the relationship between the amplitude and maximum wave height when the primary mode is 0.60Hz. Looking at the time of vibration control, it can be seen that the maximum wave height and amplitude are proportional. Furthermore, it can be seen that the rate of increase of the maximum wave height is moderated by adding a damping device, and the maximum wave height is reduced here as well. The damping constant is summarized in Table 2.

Photo 5 shows an internal photo with 0.60 Hz, ± 10 mm attenuation, and Photo 6 shows an internal photo with 0.60 Hz, ± 10 mm attenuation. Comparing these photos, it can be seen that the camera is covered with water in the case of non-vibration suppression in Photo 5, but the camera is not covered with water during the vibration suppression in Photo 6, and the wave height can be suppressed. b) Wall displacement

Fig. 7 shows the wall displacement when the primary mode is 0.60Hz and ± 5mm. In non-damping suppression, the wall displacement is +1.0 mm at maximum, -1.1 mm at the next valley, and wall displacement with an amplitude of 2.1 mm. On the other hand, with the addition of a damping device, the wall displacement is + 1.0mm at the maximum, -1.0mm at the next valley, and the amplitude is 2.0mm, a reduction of about 5%.

Fig. 8 shows the wall displacement when the primary mode is 0.60Hz and ± 7mm vibration is applied. In non-damping control, the maximum wall displacement is + 1.4mm, the next valley is -1.4mm and the amplitude is 2.8mm. On the other hand, with the addition of a damping device, the wall displacement is reduced by a maximum of + 1.2mm, -1.2mm in the next valley, and 2.4mm in amplitude, which is reduced by approximately 15%.

Fig. 9 shows the wall displacement when the primary mode is 0.60Hz and ± 10mm. In non-damping, wall displacement is maximum + 2.0mm, -1.7 mm and the amplitude is 3.7 mm. On the other hand, with the addition of a vibration control device, the wall displacement is reduced by about 16%, up to + 1.5mm, -1.6mm in the next valley, and 3.1mm in amplitude.

When the vibration is stopped, the wall displacement continues without attenuation in non-vibration, whereas the wall displacement converges quickly when a damping device is added. This is thought to be due to the fact that the sloshing behavior of the inner solution converged early, and the wall displacement could be suppressed.

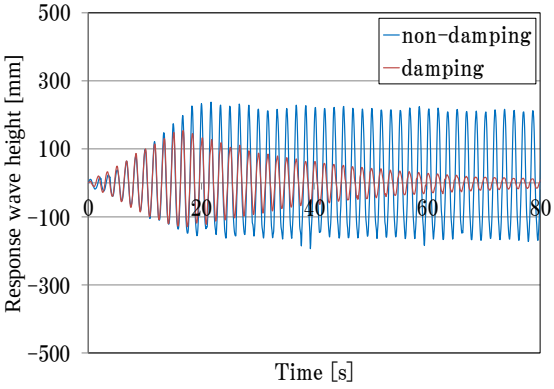

Fig. 3 ± 5mm excitation

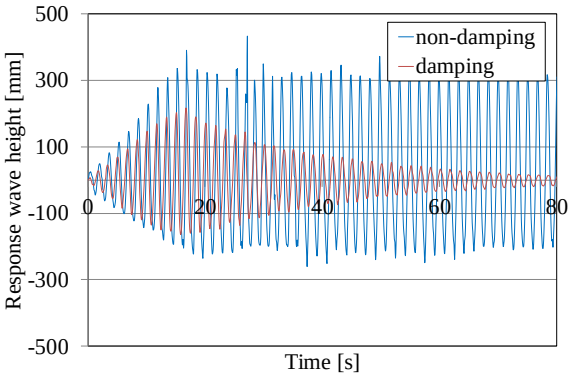

Fig. 4 ± 7mm excitation

Response wave height in primary mode

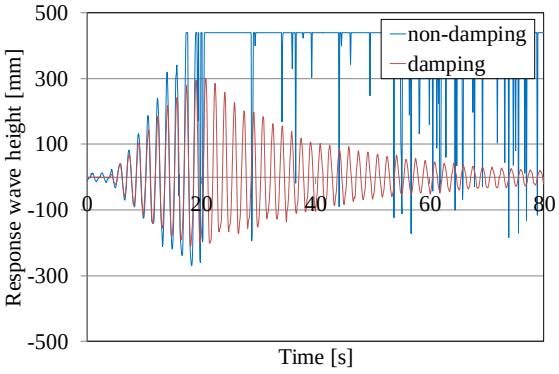

Fig. 5 ± 10mm excitation
Response wave height in primary mode

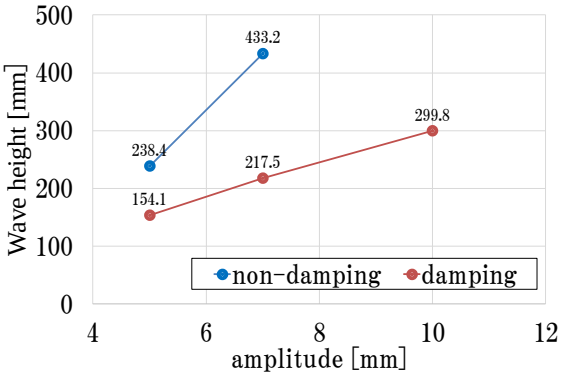

Fig. 6 Amplitude and maximum wave height during primary mode excitation

Table 2 Attenuation constant when the excitation amplitude is changed

Excitation amplitude	non-damping	damping
±5mm	0.0010	0.010
±7mm	0.0015	0.011
±10mm		0.012

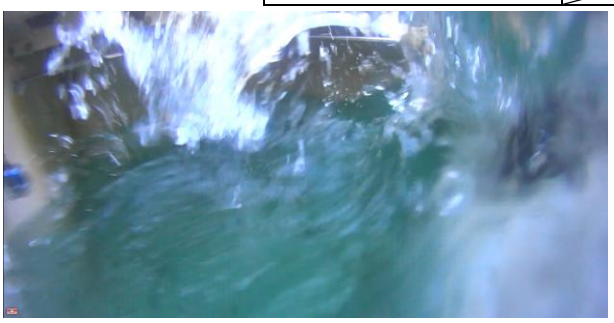

Photo 5 Non-damping of ± 10mm

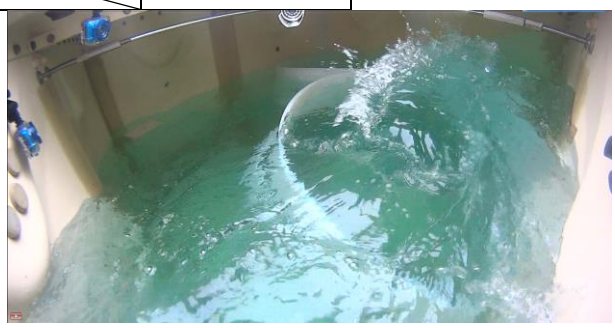

Photo 6 Damping of ± 10mm

c) Dynamic fluid pressure distribution

Fig. 10 shows the dynamic fluid pressure distribution on the wall surface when the primary mode is 0.60Hz. It can be seen that the value of the dynamic fluid pressure increases near the water surface. This indicates the characteristic of sloshing in which the inner solution acts locally near the water surface in the first mode

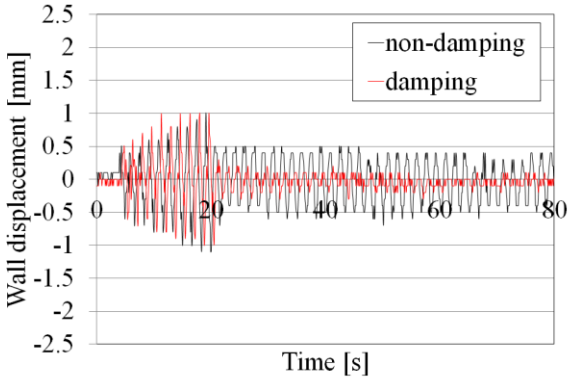

Fig. 7 ± 5mm excitation

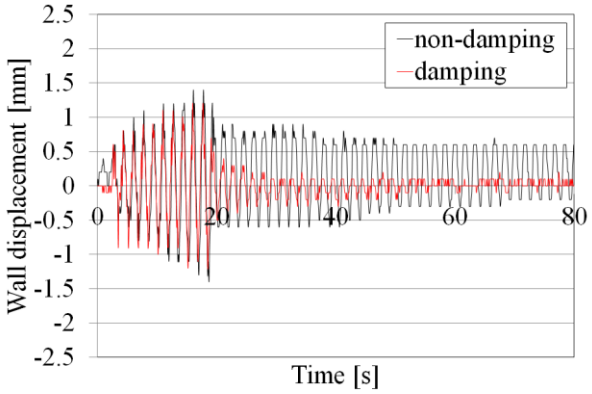

Fig. 8 ± 7mm excitation

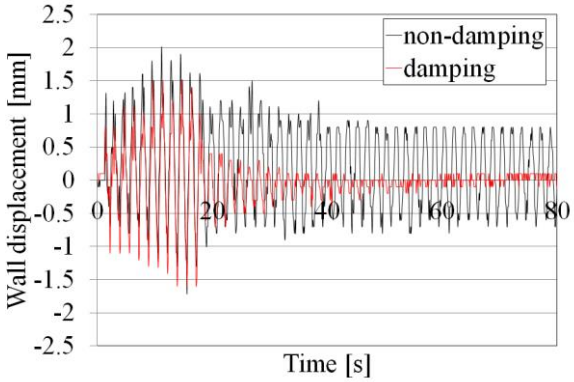

Fig. 9 ± 10mm excitation

Wall displacement

excitation. Comparing the solid line non-damping device and the broken line damping device with an excitation amplitude of ± 10mm, the non-damping was 2.2kPa at the pressure gauge installation position of 1400mm. This is the result of controlling the fluid fluctuation of sloshing behavior with a damping device.

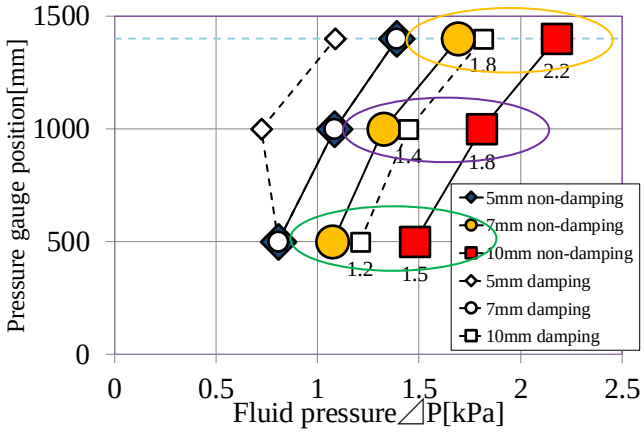

Fig. 10 Dynamic pressure distribution on wall surface during primary mode 0.60Hz excitation

4.2 Kobe NS wave 56% equivalent excitation

JMA Kobe NS direction observation wave observed at Kobe Ocean Meteorological Observatory during the Hyogoken-Nanbu Earthquake will be conducted. Here, we tried to input Kobe NS wave, but due to the capacity of the large vibration device, the vibration of the output shaking table displacement was equivalent to maximum 56%.

The maximum acceleration and seismic intensity class during excitation under the set conditions here are equivalent to 410 Gal at a Kobe NS wave displacement of 56% and a seismic intensity of about 6+. The seismic intensity class for the maximum acceleration is based on the “Method of calculating seismic intensity” in the JMA official website. The acceleration power spectrum is shown in Fig.11.

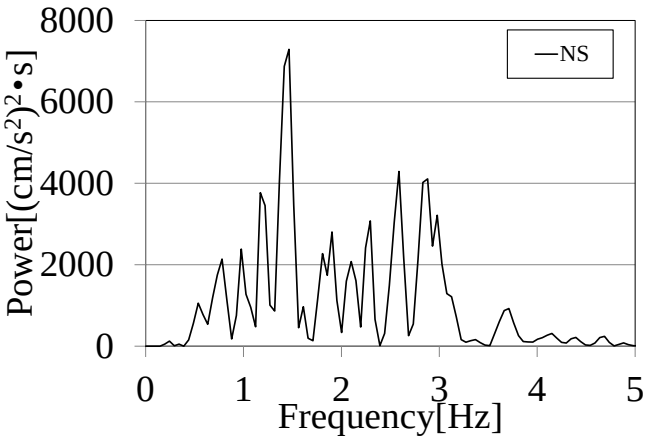

Fig. 11 Acceleration power spectrum of Kobe NS wave

a) Response wave height

Fig. 12 shows the response wave height when the Kobe NS wave is equivalent to 56%. The maximum wave height is 434 mm for non-damping, but by adding a damping device, the maximum wave height is 276 mm, about 36% reduction. In addition, from the response waveform shown in Fig. 12, by adding a vibration control device, it converges immediately after the vibration is stopped. The damping constant calculated from this result increased by approximately 4.0 times to 0.0051 for non-damping and 0.0203 for damping.

Photo 7 and Photo 8 show the non-attenuation effect equivalent to 56% of Kobe NS wave. Comparing these photos, the non-damping in Photo 7 indicates that the camera is very exposed to water, but the damping in Photo 8 is not.

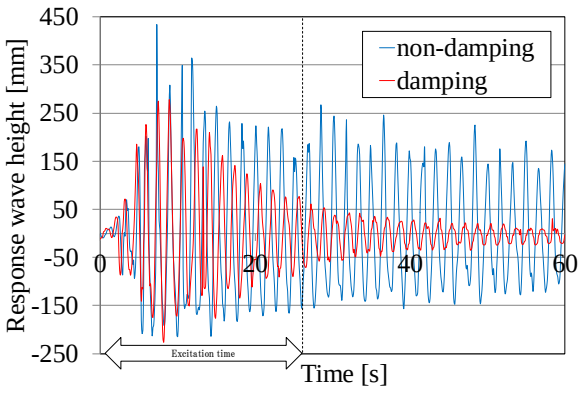

Fig. 12 Response wave height during excitation equivalent to 56% of Kobe NS wave

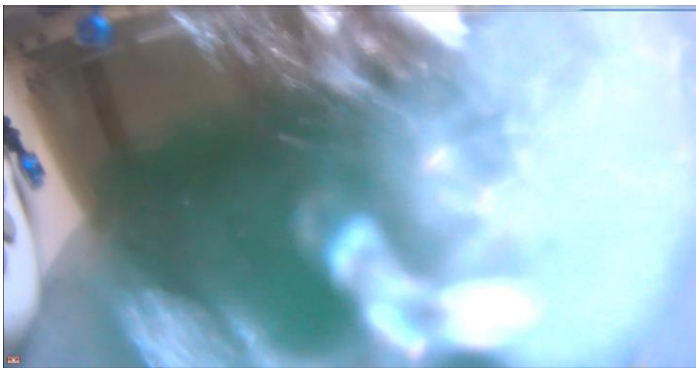

Photo 7 Non-damping 56% Kobe NS wave

Photo 8 Damping 56% Kobe NS wave

b) Wall displacement

Fig. 13 shows the wall displacement during vibration equivalent to 56% of Kobe NS waves. The non-damping, wall displacement is +11.0 mm at maximum and -3.2 mm, and the wall displacement is 14.2 mm in amplitude. Compared with this result, the wall displacement was +7.6 mm and -5.2 mm at the maximum, and the wall displacement of 12.8 mm in amplitude was reduced by about 10% during damping. On the other hand, if attention is paid after the vibration is stopped, the continuation of the non-damping wall surface can be quickly converged by adding the damping device, preventing the tank from being damaged.

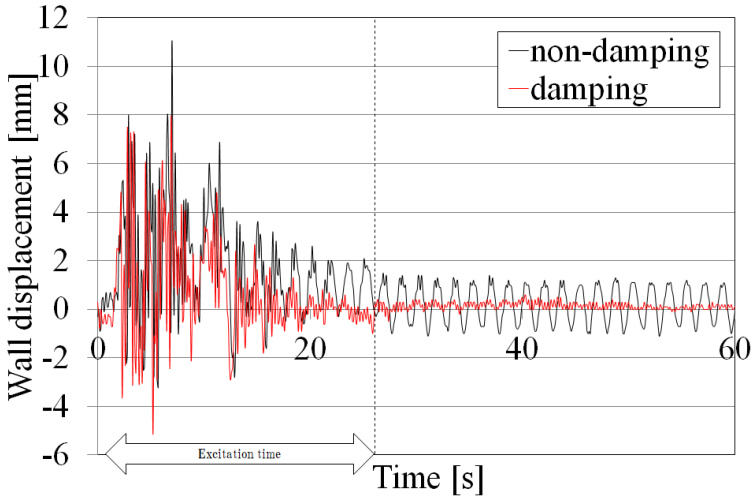

Fig. 13 Wall displacement during excitation equivalent to 56% of Kobe NS wave

c) Fluid pressure distribution

Fig. 14 shows the distribution of dynamic fluid pressure on the wall surface during vibration equivalent to 56% of Kobe NS waves. It can be seen that the values of the dynamic fluid pressure distribution increase as the pressure gauge installation position approaches the bottom surface, unlike the case of primary mode sine wave excitation. In addition, the fluid pressure distribution is swollen. This is thought to be due to seismic excitation, a characteristic resembling the bulging behavior in which the wall is coupled with the internal solution. Comparing the non-damping with the solid line and the damping suppression with the broken line, the pressure gauge installation positions of 1000mm and 500mm, which were 7.6kPa and 8.5kPa, respectively, moved to 5.1kPa and 7.0kPa by adding a damping device. The value of fluid pressure change is reduced. In addition, the non-damping and bulging dynamic fluid pressure distribution becomes a linear distribution during vibration suppression by reducing the sloshing response wave height, reducing the acceleration response load due to the fluctuation of the content liquid, and reducing the bulging behavior. we guess it may have led to a reduction in the dynamic fluid pressure change. However, this needs to be confirmed again in the future.

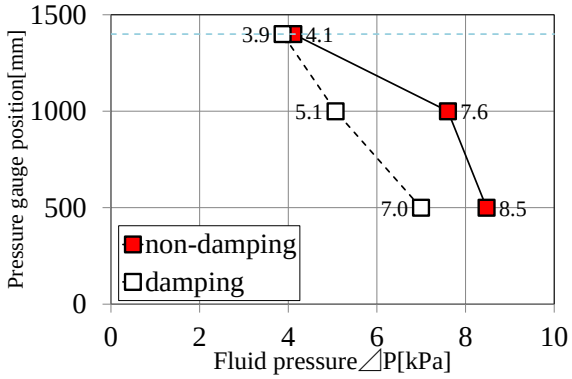

Fig. 14 Dynamic pressure distribution on wall surface during vibration equivalent to 56% of Kobe NS wave

5. Conclusion

This paper attempted to reduce the damage by installing a vibration control device inside the water tank, considering that the water tank was damaged due to the sloshing phenomenon of the solution in the tank during the earthquake. Here, a vibration experiment using a real water storage tank made of 2 × 2 × 2mFRP was conducted, and the effect of the 8-shaped floating damping device proposed in this paper was verified.

When the 8-shaped floating damping device was installed, the maximum wave height was reduced by 35-50% in the sinusoidal primary mode excitation. It was confirmed that the damping constant was 0.010 to 0.012, approximately 8 to 10 times. In addition, the same damping effect was confirmed when the Kobe NS earthquake wave was input. Furthermore, it was suggested that the change in dynamic fluid pressure due to sloshing during sine wave excitation and seismic wave excitation was reduced. As a result, it is judged that the proposed 8-shaped floating damping device has a sufficient suppression effect on the sloshing phenomenon. Therefore, the proof stress of the entire water tank is increased and damage can be prevented, so that it will be possible to secure water as a lifeline in the event of an earthquake and lead to disaster reduction.

6. Future issues

Future studies include improvements such as not using connection members as much as possible with the aim of further improving workability. In addition, the water storage tank is equipped with various

components such as FPR panel, SUS panel, steel plate, etc., so that various members are installed inside the tank. Is to aim for generalization. By the way, the bulging phenomenon caused by the seismic excitation can be suppressed by adding a damping device to reduce the value of dynamic fluid pressure change. There is a high possibility that the repeated response of the internal solution will be suppressed. However, since the bulging vibration generation region is on the higher frequency side than the sloshing generation natural frequency, it is necessary to confirm the vibration experiment in this frequency region again.

Acknowledgments: We received cooperation from students in the Department of Urban Environmental Studies, Chuo University, Graduate School of Science and Engineering, Department of Urban Environmental Studies, and Aichi Institute of Technology, Department of Urban Environmental Studies, and Graduate School of Engineering. I express my gratitude here. Finally, a part of this research is supplemented by the Japan Society for the Promotion of Science, Grant-in-Aid for Scientific Research (C) (Research Representative: Hirokazu Hirano) and Chuo University Research Grants .

7. References

[1] Hirokazu Hirano, Tsuyoshi Ida, Tomoki Ishikawa (2016): Development of vibration control device for improving the earthquake resistance of existing water tanks, Proceedings of the 7th Infrastructure Lifeline Disaster Reduction Symposium.

[2] Ryosuke Inoue, Touichi Sakai, Shuichi Ohmine (2015): Analysis of the relationship between wide area damage of the aquarium and earthquake motion characteristics in the 2011 off the Pacific coast of Tohoku Earthquake, Journal of Japan Society of Civil Engineers, A1 (Structure and Earthquake Engineering), Vol. 71, No. 4, pp. 764-773.

[3] Ministry of Health, Labor and Welfare, Health Bureau, Water Section (2012): Great East Japan Earthquake Water Facility Damage Situation Report (2011 Disaster Assessment Documents Organized).

[4] Kunio Mizukami (2012): For the Great East Japan Earthquake -Water Tank Damage-, Saitama Architectural Design Supervision Association Bulletin, No.110, pp.10-15.

[5] Living Amenity Association Water Tank Committee (2012): Survey of water tanks after the Great East Japan Earthquake, ALIA NEWS, No. 128, pp.4-9.

[6] Tokyo Electric Power Company (2008): Kashiwazaki-Kariwa Nuclear Power Station Units 1-7 Units on flooding in the reactor building operating floor, Sound Committee No. 10-5, Reference Material 1.

[7] Fire Research Institute (2003): Fire Cause Investigation Report on Idemitsu Kosan Co., Ltd. Hokkaido Refinery crude oil tank fire that occurred in the 2003 Tokachi-oki earthquake.

[8] Touichi Sakai (2004): Regarding the damage of floating roof tanks in the 2003 Tokachi-oki earthquake, Japan Steel Structure Association, JSSC, No. 52.

[9] Tsuyoshi Ida, Hirokazu Hirano, Shinpei Arita, Naotsugu Sato, Tetsuo Okumura (2007): A study of storage tank floating roof behavior when sloshing occurs-Vibration experiment with φ4000 tank model, JSCE Proceedings A, Vol.63, No .3, pp.444-453.

[10] Shinsaku Zama, Minoru Yamada, Haruki Nishi, Mikihiro Hirokawa, Hirokazu Hirano, Moriaki Suzuki (2006): Calculation of overflow of internal solution due to sloshing of oil tank, Report of Fire Research Institute, No. 101, pp.14-20.

[11] Michiya Sakai, Sadanori Higashi, Kiyotaka Sato, Nobukazu Tanaka (2007): Nonlinear Sloshing Evaluation of Rectangular Aquarium with Overflow, Journal of Structural Engineering, Vol.53, pp.597-604.

[12] Ryuta Sone, Taisuke Ono, Tsuyoshi Ida, Hirokazu Hirano, Naotsugu Sato (2013): Examination of anti-sloshing measures in rectangular cross-section water tanks, Special Issue on A2 Volume (Applied Mechanics), Japan Society of Civil Engineers, Vol.16, pp. 833-843.

[13] Taisuke Ono, Ryuta Sone, Tsuyoshi Ida, Hirokazu Hirano, Naotsugu Sato (2015): Development of floating vibration control device for sloshing in receiving tank, JSCE A2 (Applied Mechanics), Vol.70, No .2, pp.621-629.

[14] Kazuki Noritake, Moriaki Suzuki, Tetsuo Okumura, Koichiro Saguchi, Susumu Kurahashi (2012): Examination of sloshing behavior and its suppression method in rectangular storage tank, Vol.15, pp.785-794.

